Trabecular Bone Failure at the Microstructural Level

Ralph Müller, PhD, and G. Harry van Lenthe, PhD

Corresponding author
Ralph Müller, PhD
Institute for Biomedical Engineering, University and ETH Zürich, Moussonstrasse 18, 8044 Zürich, Switzerland.
E-mail: ralph.mueller@ethz.ch

Current Osteoporosis Reports 2006, **4:**80–86
Current Science Inc. ISSN 1544-1873

Although biomedical imaging technology is now readily available, few attempts have been made to expand the capabilities of these systems by adding not only quantitative but also functional analysis tools combining microimaging with time-lapsed mechanical testing. An area of special interest is multiscale functional imaging of trabecular bone to assess the relative importance of bone "quality" in the assessment of the mechanical competence of bone. First, relevant studies dealing with hierarchical imaging of trabecular bone and classic analyses such as quantitative morphometry and finite-element analysis to predict bone strength are reviewed. Second, studies are presented investigating failure mechanisms of three-dimensional trabecular bone through dynamic, time-lapsed microimaging, including image-guided techniques developed for this purpose and utilizing microcompression. For the first time, these allow the direct three-dimensional visualization and quantification of failure initiation and progression at the microstructural level.

Introduction

The principal function of skeletal bones is to withstand the loads and moments that are placed upon them. When these loads exceed the bone tissue's ability to support them, fractures inevitably occur. In individuals with osteoporosis, fractures can occur without a singular traumatic event; thus early detection of bone loss—a skeleton at risk—will allow more prompt and appropriate treatment and ultimately improve our ability to prevent fractures. Osteoporosis is defined as a skeletal disorder characterized by compromised bone strength, predisposing to an increased risk of fracture [1]. Hence, osteoporosis would be best diagnosed by in vivo measurements of bone strength. The present "gold standard" of determining bone strength is a functional, mechanical test. Direct mechanical testing is a straightforward procedure but it is limited by its destructiveness. Therefore, this method is not applicable in vivo, and although it can be used in vitro, a sample can only be tested once, which limits the assessment of direction-dependent failure characteristics. Furthermore, these tests are prone to errors related to boundary artifacts and to the size of the specimens, which are often so small as to hamper high-precision measurements [2–4].

Bone mineral density (BMD) measurements are frequently used as a surrogate measure of bone strength. Significant correlations between apparent bone density and various mechanical properties have been demonstrated for large populations using power–law regressions [2,5,6]. On average, about 70% of the variability in bone strength in vitro is determined by its density [7]. However, the relationship between changes in bone density and changes in fracture risk is unclear. A 40% to 50% reduction in the risk of fracture through supplementation with calcium and vitamin D has been reported, although BMD increased by only 1% [8,9]. In contrast, a marked increase in BMD as a result of fluoride treatment did not decrease the risk of fracture [10]. On an individual basis, the predictive capacity of bone density seems to be even more limited. BMD explained only 4% to 28% of the 35% to 50% reduction in vertebral fracture risk after antiresorptive treatment [11–13], and although many older persons may lose bone, as expressed by a decrease in BMD, not all develop fractures [14,15]. Furthermore, individuals who have had a previous fracture are at an increased risk for future fractures, independent of BMD [16].

These findings all contribute to the notion that bone density has limitations as a surrogate for bone strength and fracture risk. This is not surprising: BMD, bone geometry, bone microarchitecture, and the bone material characteristics are all components that determine bone strength as defined by the bone's ability to withstand loading. Neuromuscular function and environmental hazards influencing the risk of falling are also important factors in determining fracture risk. As a result, it has been found that on an individual basis, 10% to 90% of the variation in the strength of trabecular bone cannot be explained by bone density [7]. Alternatively, several studies have shown that bone microarchitecture

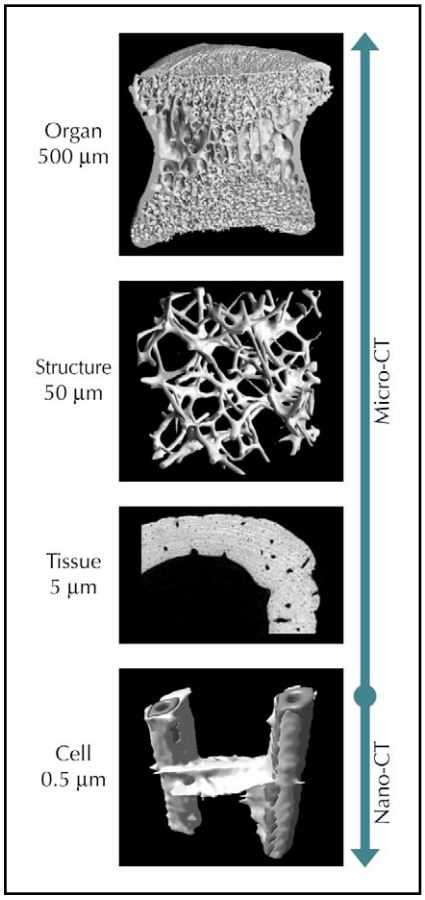

Figure 1. Schematic overview of hierarchical imaging. From top to bottom, **Organ,** cut through vertebral body demonstrating the large heterogeneity in the vertebra (desktop micro-CT); **Structure,** three-dimensional representation of the trabecular microarchitecture in a vertebral sample (desktop micro-CT); **Tissue,** cortical bone sample of a mouse femur illustrating vascular channels (large holes) and cell lacunae (synchrotron radiation micro-CT); **Cell,** fibroblast stretching between two polymer yarn filaments (synchrotron radiation micro-CT).

strongly influences its stiffness and strength, and predictions of trabecular bone competence can be greatly improved by including architectural parameters in the analysis [17–19]. Nevertheless, few attempts have been made to expand the capabilities of these systems by adding both quantitative and functional analysis tools combining bone architecture microimaging with time-lapsed mechanical testing.

This article reviews strategies for new three-dimensional (3-D) approaches for functional imaging in the study of osteoporosis and bone loss. The focus is on hierarchical assessment of trabecular bone failure using a combined experimental and computational approach. With the introduction of microstructural imaging systems such as desktop micro-CT, a new generation of imaging instruments has entered the arena, allowing easy access to the 3-D microstructure of bone and giving researchers a powerful tool for the exploration of hierarchical relationships between structure and function in age-related bone loss and osteoporosis.

Three-Dimensional Imaging of Bone Microarchitecture

Traditionally, trabecular bone morphometry has been assessed in two dimensions. The structural parameters are either inspected visually or measured from sections, and the third dimension is added on the basis of stereology [20]. To overcome some of the limitations of two-dimensional histology, several 3-D measurement and analysis techniques have been developed over the past two decades. The most common is the use of stereo microscopy or scanning microscopy to qualitatively assess 3-D microstructure. Using these methods, researchers have been able to demonstrate the loss of 3-D connectivity with age by visual observation [21]. Serial sectioning also has been employed to explore the third dimension quantitatively, allowing true measurements of connectivity and other 3-D structural properties such as volume fraction and surface area [22]. Nevertheless, because it is truly destructive, serial sectioning techniques will not allow secondary measurements such as mechanical testing or dynamic histomorphometry.

An ideal imaging approach would be hierarchical, volumetric (3-D), multi-contrast (hard vs soft tissue), and, above all, fully noninvasive. Hierarchical imaging denotes the ability to resolve anatomic features at a variety of resolutions and size scales using basically the same imaging modality and ideally covering a few orders of magnitude in resolution. This ability will allow measurements starting at the organ level (500 µm resolution) and going down from the structural level (50 µm) to tissue level (5 µm), and even to the cell level (0.5 µm) using the same technology (Fig. 1).

One such approach to imaging and quantifying trabecular bone in three dimensions is CT scanning, which provides multiscale biologic imaging capabilities with isotropic resolutions ranging from a few millimeters (clinical CT) to a few tens of micrometers (micro-CT) down to 100 nanometers (synchrotron radiation nano-CT). Early implementations of 3-D micro-CT focused on the methodologic aspects of the systems and required equipment that was not widely available [23]. Recent developments have emphasized the practical aspects of microtomographic imaging [24]. This and other similar types of systems, now also commercially available, can be used routinely in basic research and clinical laboratories. Also known as desktop micro-CT, these systems provide nominal resolutions ranging from roughly 5 to 100 µm. Specimens with diameters ranging from a few millimeters to 100 mm can be measured. Desktop micro-CT is a precise and validated technique [25–29], which has been used extensively for research projects involving bone microarchitecture [29–34] and biomaterials [35,36]. Since the introduction of these systems, there has been increasing demand for microtomographic technology throughout the world.

Quantification of Bone Microarchitecture

In terms of understanding the basic structure types that exist in trabecular bone, simple models have been proposed. A common distinction is the division into rodlike and platelike bone structures. These highly idealized models can be considered to be two ends of a spectrum; the architecture of a real bone specimen will be a mixture of both rods and plates. The prevalence of these types depends on the anatomic site and the bone age, with typical progression from a platelike to a rodlike structure.

A method of quantitatively describing bone architecture and the changes associated with age or stage of a disease is the calculation of morphometric indices, also referred to as quantitative bone morphometry. In the past, structural properties of trabecular bone were investigated by examining two-dimensional sections of bone biopsies. Three-dimensional morphometric parameters were then derived from the two-dimensional images using stereological methods [20]. Highly significant correlations between two-dimensional histology and 3-D micro-CT have been found for bone volume density (BV/TV) and bone surface density (BS/TV), where BV stands for bone volume, BS for bone surface, and TV for total volume [37]. Although measurements like BV/TV and BS/TV can be obtained directly from two-dimensional images, a range of important parameters such as trabecular thickness (Tb.Th), trabecular separation (Tb.Sp), and trabecular number (Tb.N) are derived indirectly, assuming a fixed-structure model. Typically, an ideal plate or ideal rod model is used. Such assumptions are unreliable because trabecular bone architecture differs at different sites and continuously changes its structure as a result of remodeling. This problem was demonstrated clearly in a large study of 260 human bone biopsies taken from five different skeletal sites and evaluated with both traditional two-dimensional histomorphometry and newly developed 3-D methods [38]. For Tb.Th, Tb.Sp, and Tb.N, marked differences between the two methods were found and correlations were only moderate. Because of anatomic differences in bone architecture, correlations varied according to anatomic site. The discrepancy between the true trabecular architecture and the assumed structure will be larger for one site than for another site. Hence, deviation from the assumed model will lead to an unpredictable error of the indirectly derived parameters, particularly in studies that follow the changes in bone structure in the course of age-related bone loss and those that evaluate drug therapy. In such cases, a predefined model assumption could easily overestimate or underestimate the effects of the bone atrophy, depending on the assessed index.

For these reasons, and in order to take full advantage of the volumetric measurements, several new 3-D image processing methods have recently been presented, allowing direct quantification of bone microarchitecture [22,38]. These techniques calculate actual distances in 3-D space; because they do not rely on an assumed model type, they are not biased by possible deviations. In addition to the computation of direct metric parameters, nonmetric parameters can be calculated to describe the 3-D nature of a bone structure. An estimation of the plate-rod characteristics can be achieved using the structure model index (SMI) [39]. For an ideal plate structure, the SMI is 0; for an ideal rod structure, the SMI is 3. For a structure with both plates and rods, the value will be between 0 and 3. Another parameter often used as an architectural index is geometric or structural anisotropy [40], a measure of the primary orientation of the trabeculae, often referred to as *degree of anisotropy* (DA).

Quantitative assessment of 3-D trabecular bone morphometry applies to porous structures as a whole, not to their individual elements. Although studies demonstrate the importance of architectural bone properties in a statistical sense, they do not explain the real physical contribution of the microarchitecture to the mechanical failure behavior of bone. A recent project aimed to calculate the structural properties of individual trabecular elements [41]. The ability to break down the bone microarchitecture and extract individual structural elements, such as trabecular rods and plates, allows *local* bone morphometry—that is, determination of the shape and form of each individual bone element. It is then possible to quantify individual trabeculae with respect to their volume, thickness, orientation, and type of structure, as well as their contribution to mechanical competence. In a recent study, local bone morphometry was performed on a large number of human vertebral bone samples and was compared to bone stiffness [42]. A multiple linear regression model combining mean trabecular spacing, mean slenderness of the rods, and the relative amount of rod volume to total bone volume was able to explain 90% of the variance in bone stiffness. This model could not be improved by adding bone volume density as an independent variable. Furthermore, it was found that mean trabecular thickness of the rods was significantly related to bone stiffness (r^2 = 0.42), whereas mean trabecular thickness of plates had no correlation to stiffness. Globally determined trabecular thickness, which, as classically assessed, does not discriminate between rods and plates, had poor predictive power for bone stiffness (r^2 = 0.09), demonstrating the importance of local analysis of individual rods and plates.

Experimental Assessment of Bone Competence

Although high-resolution imaging is of great value in assessing age-related bone loss and the effects of interventions on bone microarchitecture, the ultimate aim of any bone measurement in patients is to assess bone strength. The gold standard to determine bone competence is direct mechanical testing of bone. Although it is a straightforward procedure, care must be taken in interpreting the results, which are influenced by anatomic site and loading direction and can be affected to a large extent by end-artifacts

[2,3]. Mechanical testing has shown huge heterogeneity in bone mechanical properties, and not only across sites and specimens. Even within the same bone, these properties can differ 50-fold. Testing has also shown that bone is not equally strong in all directions. This mechanical anisotropy is expressed as the ratio of the stiffness in the strongest direction to the stiffness in the weakest direction, and can range from basically 1 (no preferential orientation) to over 10 for both stiffness and strength [43–45]. Because the mechanical behavior of trabecular bone is largely determined by its architecture, many investigators have correlated structural parameters with mechanical properties. Several studies have shown that bone density alone explains about 70% of bone elastic properties, but including structural anisotropy increases the predictive power to over 90% [17–19].

All these studies were performed on excised bone specimens. In a recent study [46], we showed for the first time that the inclusion of bone architectural indices is also beneficial for predicting the mechanical competence of whole bones. We evaluated the effect of ibandronate on bone mass, architecture, and strength in a study of 61 ovariectomized adult macaques. The macaques were divided into five groups (n = 11–15): sham control, ovariectomized control, and ovariectomized low-, medium-, and high-dose ibandronate. We showed that, in pooled populations, bone mass, as assessed by BV, is the single most important predictor for ultimate load ($r^2 = 0.67$). In stepwise multiple regression analysis, Tb.Sp, SMI, and BS/BV contributed an additional 21% independently of BV, so that a total of 88% of the mechanical-structural relationship was explained.

Image-Based Assessment of Bone Competence

Although the inclusion of architectural parameters has strongly improved the prediction of strength for bone specimens [19], this occurs only in a statistical sense. These parameters do not explain the real physical contribution of the microarchitecture to the mechanical failure behavior of bone. To understand how differences in bone microarchitecture influence bone strength, insight into load transfer through the bone architecture is needed. With the advent of fast and powerful computers, simulation techniques are becoming popular for investigating the mechanical properties of bone.

Microstructural finite-element analysis

Using microstructural finite-element (μFE) models generated directly from computer reconstructions of trabecular bone, it is now possible to perform a "virtual experiment"—that is, to simulate a mechanical test in great detail and with high precision. Detailed FE models of trabecular bone can be created using 3-D microstructural images, as previously described. They are often denoted as "high-resolution," "large-scale," or "microstructural" FE models. These models typically represent small trabecular cubes measuring 5 to 10 mm, a scale at which the bone behaves as a continuum. After assigning appropriate material properties to the elements defining the structure, these computer models provide realistic response characteristics to simulated loading. For linear deformation conditions, a comparison of biomechanical compression tests and μFE models shows very good agreement when a homogeneous, isotropic tissue modulus is applied [47,48]. This result holds true for both normal and osteoporotic bone [49]. These computer models allow calculation of loads at the microstructural level or even the tissue level [48,50] and have been used extensively to accurately determine the apparent mechanical properties of bone specimens.

Recently, it has been shown that these μFE models can also accurately predict trabecular bone failure for both bovine [51••] and human [52] trabecular bone. The μFE predictions of apparent stresses and strains at failure were equal to experimentally measured values for the same bone specimens, demonstrating that the quality of μFE analyses has reached such accuracy that the use of such simulation techniques can be an effective way to reduce experimental errors [18] and can be used as an alternative to destructive mechanical tests [51••]. A great advantage of μFE analysis is that the models can be analyzed many times under different conditions to simulate various types of loading. Furthermore, bone μFE models provide better insight into the relationship of structure and strength by allowing us to look inside the bone to see where stresses are localizing and therefore where they may cause fracture [53].

Image-guided failure assessment

Thus far, μFE models have mainly assessed bone loading in the elastic range, based on the notion that bone strength is highly correlated with its elastic properties [44,54]. However, bone fracture is a time-dependent, nonlinear event that includes high local deformations and local trabecular fractures. Although some work on bone failure characteristics has been done, basic knowledge of local trabecular failure is still lacking. In estimating the risk of spontaneous fractures, an extended understanding of the failure behavior of trabecular bone is essential.

For this reason, our group has developed an image-guided technique allowing direct, time-lapsed, 3-D visualization and quantification of fracture progression on the microscopic level [55•]. This technique has recently been validated in comparison with classic, continuous mechanical testing [56••]. Additionally, novel image analysis approaches have been developed in order to identify and classify individual rods and plates, to track those elements over the time course of failure, and eventually to compute local displacements and strains from consecutive compression steps [57]. This new method uses sequential structural images from stepwise microcompression testing to 1) align all images from the

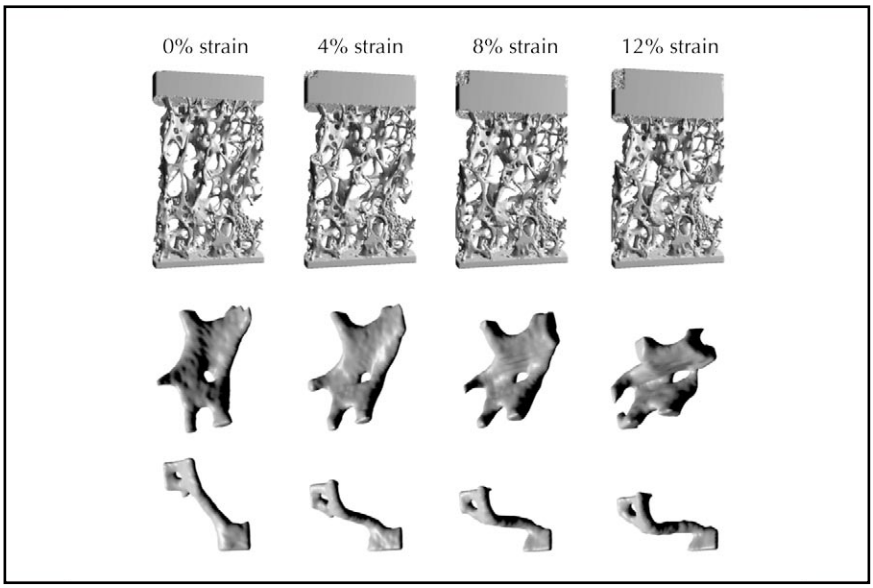

Figure 2. Failure assessment in a human spine sample using time-lapsed tomographic imaging. **Top row,** Compressed specimen, imaged in steps of 4% strain. **Middle row,** How microcompression can be used to noninvasively monitor the deformation of individual plate elements. **Bottom row,** How microcompression can be used to noninvasively monitor the deformation of individual rod elements.

various steps; 2) identify local anatomic features (nodes) in the structure, which can be followed directly in the structure throughout all the steps; 3) create a network of connections between those nodes by image decomposition; and 4) compute nodal displacements and local strains between the nodes.

In an initial study, trabecular bone specimens were compressed in steps of 0%, 1%, 2%, 4%, 8%, and 12% and local strains were determined experimentally. The method was validated using images that contained only translations or a uniform stretch in the direction of compression. For the translation, our method predicted the correct translations and the computed strains were zero, as expected. For the uniformly stretched images, we computed strain averages close to the stretch factor (< 1% error) with a standard deviation of about 10%. For the actual bone microcompression tests, the results showed that average strains were much smaller than the externally applied strain, but maximum local strain values were five to eight times greater than the externally applied strain, providing further evidence for a bandlike, local failure behavior of trabecular bone (Fig. 2). These strains were found in rod-like elements that were aligned with the main strain axis. Some of these elements bend, others buckle, and some are compressed. Although internode strains can indicate active structure elements, they cannot distinguish the different behavior of these elements and how much energy is absorbed. They also do not correlate well with the amount of deformation in an element. Therefore, internode strains alone cannot fully explain the failure mechanisms of trabecular bone.

Recently, histologic damage labeling, micro-CT imaging, and image-based finite-element analysis were combined to detect regions of trabecular bone microdamage [58•]. For the purpose of the study, bovine tibial trabecular bone cores underwent a stepwise, uniaxial compression routine in which specimens were micro-CT imaged following each compression step. Regions of trabecular bone microdamage were then registered to estimated microstructural stresses and strains. The results indicate that the mode of trabecular failure observed by micro-CT imaging agrees well with the polarity and distribution of stresses within an individual trabecula as assessed from finite-element analysis. Analysis of on-axis subsections within specimens provided significant positive relationships between microdamage and estimated tissue stress and strain. In a more localized analysis, individual microdamaged and undamaged trabeculae were extracted from specimens loaded within the elastic region and to the apparent yield point. As expected, damaged trabeculae in both groups showed significantly higher local stresses and strains than undamaged trabeculae [58•].

Bone Breaks at Its Weakest Link

Image-guided failure assessment has shown that failure of an individual trabecula can lead to global bone failure; hence, bone failure can be best predicted using a "weakest link of the chain" approach [59]. Local bone morphometry allows identification of "weak" trabeculae and therefore improves the predictive ability to determine bone strength and failure behavior. A 10% change in local thickness (in the rods only) was found to be responsible for a three-fold increase in the mechanical strength of osteoporotic bone, whereas changes in bone density were only linearly related to bone strength. This might explain a number of findings in which small changes in bone density could produce up to 70% reduction in the incidence of fracture. If it were possible to preferentially treat the weakest links of the structure, a minor increase in individual element quality, rather than large quantities of new bone, might be enough to prevent a fracture. At this time, however, this idea is purely speculative because there are no data from treated patients, although it will

be possible to obtain such data from iliac bone samples of real patients undergoing treatment. The ability to analyze the same bone sample using both noninvasive microarchitectural imaging and mechanical testing is likely to cause a revival in the use of iliac bone biopsies in the initial assessment of therapeutic success and the regulatory approval of new drugs.

Conclusions

Microarchitectural bone imaging is a nondestructive, noninvasive, and precise procedure that allows the measurement of trabecular bone as well as the repetitive 3-D assessment and computation of microstructural and micromechanical properties in patients. The procedure can help improve predictions of fracture risk, clarify the pathophysiology of skeletal diseases, and define the response to therapy. Hierarchical bioimaging, in combination with biocomputational approaches, is well suited to the investigation of structure-function relationships and trabecular failure mechanisms in normal, osteoporotic, and treated bone. We expect these findings to improve our understanding of the influence of densitometric, morphologic, and loading factors in the etiology of spontaneous fractures of the hip and the spine. Eventually, this improved understanding may lead to more successful approaches for the prevention of such fractures.

References and Recommended Reading

Papers of particular interest, published recently, have been highlighted as:

- • Of importance
- •• Of major importance

1. *Osteoporosis prevention, diagnosis, and therapy (NGC-1761)*. Bethesda, MD: National Institutes of Health (NIH); 2000.
2. Odgaard A, Linde F: **The underestimation of Young's modulus in compressive testing of cancellous bone specimens.** *J Biomech* 1991, **24:**691–698.
3. Keaveny TM, Pinilla TP, Crawford RP, et al.: **Systematic and random errors in compression testing of trabecular bone.** *J Orthop Res* 1997, **15:**101–110.
4. Jamsa T, Jalovaara P, Peng Z, et al.: **Comparison of three-point bending test and peripheral quantitative computed tomography analysis in the evaluation of the strength of mouse femur and tibia.** *Bone* 1998, **23:**155–161.
5. Carter DR, Hayes WC: **The compressive behavior of bone as a two-phase porous structure.** *J Bone Joint Surg Am* 1977, **59:**954–962.
6. Rice JC, Cowin SC, Bowman JA: **On the dependence of the elasticity and strength of cancellous bone on apparent density.** *J Biomech* 1988, **21:**155–168.
7. Wehrli FW, Saha PK, Gomberg BR, et al.: **Role of magnetic resonance for assessing structure and function of trabecular bone [review].** *Top Magn Reson Imaging* 2002, **13:**335–355.
8. Chapuy MC, Arlot ME, Duboeuf F, et al.: **Vitamin D3 and calcium to prevent hip fractures in the elderly women.** *N Engl J Med* 1992, **327:**1637–1642.
9. Dawson-Hughes B, Harris SS, Krall EA, Dallal GE: **Effect of calcium and vitamin D supplementation on bone density in men and women 65 years of age or older.** *N Engl J Med* 1997, **337:**670–676.
10. Riggs BL, Hodgson SF, O'Fallon WM, et al.: **Effect of fluoride treatment on the fracture rate in postmenopausal women with osteoporosis.** *N Engl J Med* 1990, **322:**802–809.
11. Reginster J, Minne HW, Sorensen OH, et al.: **Randomized trial of the effects of risedronate on vertebral fractures in women with established postmenopausal osteoporosis. Vertebral Efficacy with Risedronate Therapy (VERT) Study Group.** *Osteoporos Int* 2000, **11:**83–91.
12. Ettinger B, Black DM, Mitlak BH, et al.: **Reduction of vertebral fracture risk in postmenopausal women with osteoporosis treated with raloxifene: results from a 3-year randomized clinical trial. Multiple Outcomes of Raloxifene Evaluation (MORE) Investigators.** *JAMA* 1999, **282:**637–645.
13. Black DM, Thompson DE, Bauer DC, et al.: **Fracture risk reduction with alendronate in women with osteoporosis: the Fracture Intervention Trial.** *J Clin Endocrinol Metab* 2000, **85:**4118–4124.
14. Melton LJ 3rd, Kan SH, Frye MA, et al.: **Epidemiology of vertebral fractures in women.** *Am J Epidemiol* 1989, **129:**1000–1011.
15. Rüegsegger P: **Bone density measurement.** In *Osteoporosis: A Guide to Diagnosis and Treatment*. Edited by Bröll H, Dambacher MA. Basel: Karger; 1996:103–116.
16. Ross PD, Davis JW, Epstein RS, Wasnich RD: **Pre-existing fractures and bone mass predict vertebral fracture incidence in women.** *Ann Intern Med* 1991, **114:**919–923.
17. Turner CH, Cowin SC, Rho JY, et al.: **The fabric dependence of the orthotropic elastic constants of cancellous bone.** *J Biomech* 1990, **23:**549–561.
18. van Rietbergen B, Odgaard A, Kabel J, Huiskes R: **Relationships between bone morphology and bone elastic properties can be accurately quantified using high-resolution computer reconstructions.** *J Orthop Res* 1998, **16:**23–28.
19. Yang G, Kabel J, van Rietbergen B, et al.: **The anisotropic Hooke's law for cancellous bone and wood.** *J Elast* 1998–1999, **53:**125–146.
20. Parfitt AM, Mathews CH, Villanueva AR, et al.: **Relationships between surface, volume, and thickness of iliac trabecular bone in aging and in osteoporosis. Implications for the microanatomic and cellular mechanisms of bone loss.** *J Clin Invest* 1983, **72:**1396–1409.
21. Mosekilde L: **Consequences of the remodelling process for vertebral trabecular bone structure: a scanning electron microscopy study (uncoupling of unloaded structures).** *Bone Miner* 1990, **10:**13–35.
22. Odgaard A: **Three-dimensional methods for quantification of cancellous bone architecture.** *Bone* 1997, **20:**315–328.
23. Feldkamp LA, Goldstein SA, Parfitt AM, et al.: **The direct examination of three-dimensional bone architecture in vitro by computed tomography.** *J Bone Miner Res* 1989, **4:**3–11.
24. Rüegsegger P, Koller B, Müller R: **A microtomographic system for the nondestructive evaluation of bone architecture.** *Calcif Tissue Int* 1996, **58:**24–29.
25. Balto K, Müller R, Carrington DC, et al.: **Quantification of periapical bone destruction in mice by micro-computed tomography.** *J Dent Res* 2000, **79:**35–40.
26. Graichen H, Lochmüller EM, Wolf E, et al.: **A non-destructive technique for 3-D microstructural phenotypic characterisation of bones in genetically altered mice: preliminary data in growth hormone transgenic animals and normal controls.** *Anat Embryol (Berl)* 1998, **199:**239–248.
27. Kapadia RD, Stroup GB, Badger AM, et al.: **Applications of micro-CT and MR microscopy to study pre-clinical models of osteoporosis and osteoarthritis.** *Technol Health Care* 1998, **6:**361–372.

28. Müller R, Hildebrand T, Hauselmann HJ, Rüegsegger P: **In vivo reproducibility of three-dimensional structural properties of noninvasive bone biopsies using 3D-pQCT.** *J Bone Miner Res* 1996, **11:**1745–1750.
29. Yamashita T, Nabeshima Y, Noda M: **High-resolution micro-computed tomography analyses of the abnormal trabecular bone structures in klotho gene mutant mice.** *J Endocrinol* 2000, **164:**239–245.
30. Alexander JM, Bab I, Fish S, et al.: **Human parathyroid hormone 1-34 reverses bone loss in ovariectomized mice.** *J Bone Miner Res* 2001, **16:**1665–1673.
31. Dempster DW, Cosman F, Kurland ES, et al.: **Effects of daily treatment with parathyroid hormone on bone microarchitecture and turnover in patients with osteoporosis: a paired biopsy study.** *J Bone Miner Res* 2001, **16:**1846–1853.
32. Müller R, Hahn M, Vogel M, et al.: **Morphometric analysis of noninvasively assessed bone biopsies: comparison of high-resolution computed tomography and histologic sections.** *Bone* 1996, **18:**215–220.
33. Turner CH, Hsieh YF, Müller R, et al.: **Genetic regulation of cortical and trabecular bone strength and microstructure in inbred strains of mice.** *J Bone Miner Res* 2000, **15:**1126–1131.
34. von Stechow D, Balto K, Stashenko P, Müller R: **Three-dimensional quantitation of periradicular bone destruction by micro-computed tomography.** *J Endod* 2003, **29:**252–256.
35. Lutolf MP, Weber FE, Schmoekel HG, et al.: **Repair of bone defects using synthetic mimetics of collagenous extracellular matrices.** *Nat Biotechnol* 2003, **21:**513–518.
36. Zeltinger J, Sherwood JK, Graham DA, et al.: **Effect of pore size and void fraction on cellular adhesion, proliferation, and matrix deposition.** *Tissue Eng* 2001, **7:**557–572.
37. Müller R, Van Campenhout H, Van Damme B, et al.: **Morphometric analysis of human bone biopsies: a quantitative structural comparison of histological sections and micro-computed tomography.** *Bone* 1998, **23:**59–66.
38. Hildebrand T, Laib A, Müller R, et al.: **Direct three-dimensional morphometric analysis of human cancellous bone: microstructural data from spine, femur, iliac crest, and calcaneus.** *J Bone Miner Res* 1999, **14:**1167–1174.
39. Hildebrand T, Rüegsegger P: **Quantification of bone microarchitecture with the structure model index.** *Comput Methods Biomech Biomed Engin* 1997, **1:**15–23.
40. Whitehouse WJ: **The quantitative morphology of anisotropic trabecular bone.** *J Microsc* 1974, **101:**153–168.
41. Stauber M, Müller R: **Volumetric spatial decomposition of trabecular bone into rods and plates—A new method for local bone morphometry.** *Bone* 2006, **38:**475–484.
42. Stauber M, Rapillard L, van Lenthe GH, et al.: **Importance of individual rods and plates in the assessment of bone quality and their contribution to bone stiffness.** *J Bone Miner Res* 2006, **21**:586–595.
43. Ciarelli MJ, Goldstein SA, Kuhn JL, et al.: **Evaluation of orthogonal mechanical properties and density of human trabecular bone from the major metaphyseal regions with materials testing and computed tomography.** *J Orthop Res* 1991, **9:**674–682.
44. Hodgskinson R, Currey JD: **The effect of variation in structure on the Young's modulus of cancellous bone: a comparison of human and non-human material.** *Proc Inst Mech Eng [H]* 1990, **204:**115–121.
45. Keaveny TM, Morgan EF, Niebur GL, Yeh OC: **Biomechanics of trabecular bone.** *Annu Rev Biomed Eng* 2001, **3:**307–333.
46. Müller R, Hannan M, Smith SY, Bauss F: **Intermittent ibandronate preserves bone quality and bone strength in the lumbar spine after 16 months of treatment in the ovariectomized cynomolgus monkey.** *J Bone Miner Res* 2004, **19:**1787–1796.
47. Kabel J, Van Rietbergen B, Dalstra M, et al.: **The role of an effective isotropic tissue modulus in the elastic properties of cancellous bone.** *J Biomech* 1999, **32:**673–680.
48. Ladd AJ, Kinney JH, Haupt DL, Goldstein SA: **Finite-element modeling of trabecular bone: comparison with mechanical testing and determination of tissue modulus.** *J Orthop Res* 1998, **16:**622–628.
49. Homminga J, McCreadie BR, Weinans H, Huiskes R: **The dependence of the elastic properties of osteoporotic cancellous bone on volume fraction and fabric.** *J Biomech* 2003, **36:**1461–1467.
50. van Rietbergen B, Weinans H, Huiskes R, Odgaard A: **A new method to determine trabecular bone elastic properties and loading using micromechanical finite-element models.** *J Biomech* 1995, **28:**69–81.
51.•• Niebur GL, Feldstein MJ, Yuen JC, et al.: **High-resolution finite element models with tissue strength asymmetry accurately predict failure of trabecular bone.** *J Biomech* 2000, **33:**1575–1583.

A bilinear constitutive model with asymmetric tissue yield strains in tension and compression was applied to simulate failure in high-resolution, finite-element models of bovine tibial specimens. Findings show that the resulting models can capture the apparent strength behavior of individual trabeculae to an outstanding level of accuracy, suggesting that computational models have reached a level of fidelity that qualifies them as surrogates for destructive mechanical testing of real specimens.

52. Bayraktar HH, Morgan EF, Niebur GL, et al.: **Comparison of the elastic and yield properties of human femoral trabecular and cortical bone tissue.** *J Biomech* 2004, **37:**27–35.
53. Borah B, Gross GJ, Dufresne TE, et al.: **Three-dimensional microimaging (MRμI and μCT), finite element modeling, and rapid prototyping provide unique insights into bone architecture in osteoporosis.** *Anat Rec* 2001, **265:**101–110.
54. Hou FJ, Lang SM, Hoshaw SJ, et al.: **Human vertebral body apparent and hard tissue stiffness.** *J Biomech* 1998, **31:**1009–1015.
55.• Müller R, Gerber SC, Hayes WC: **Micro-compression: a novel technique for the nondestructive assessment of local bone failure.** *Technol Health Care* 1998, **6:**433–444.

This study shows for the first time that trabecular bone failure can be observed in a time-lapsed fashion on the microstructural level.

56.•• Nazarian A, Müller R: **Time-lapsed microstructural imaging of bone failure behavior.** *J Biomech* 2004, **37:**55–65.

Time-lapsed microstructural imaging of bone failure behavior is introduced and validated using a novel micromechanical testing system that facilitates stepwise compression of trabecular bone specimens. The technique allows direct 3-D visualization and quantification of fracture initiation and progression on the microscopic level and relates the global failure properties of trabecular bone to those of the individual trabeculae.

57. Müller R, Boesch T, Jarak D, et al.: **Micro-mechanical evaluation of bone microstructures under load.** In *Developments in X-Ray Tomography III*, vol. 4503. Edited by Bonse U. San Diego, CA: SPIE; 2002:189–200.
58.• Nagaraja S, Couse TL, Guldberg RE: **Trabecular bone microdamage and microstructural stresses under uniaxial compression.** *J Biomech* 2005, **38:**707–716.

This study demonstrates that the combination of functional imaging and image-based finite-element analysis allows accurate prediction of regions of trabecular bone microdamage as evaluated by histologic damage labeling. More data of this type are needed to improve understanding of factors contributing to initiation of microdamage and to establish local failure criteria for normal and diseased trabecular bone.

59. Müller R: **Bone microarchitecture assessment: current and future trends.** *Osteoporosis Int* 2003, **14(Suppl 5):**S89–S99.